Advanced Review

Magnetic nanoparticle biosensors

Jered B. Haun, Tae-Jong Yoon, Hakho Lee and Ralph Weissleder*

One of the major challenges in medicine is the rapid and accurate measurement of protein biomarkers, cells, and pathogens in biological samples. A number of new diagnostic platforms have recently been developed to measure biomolecules and cells with high sensitivity that could enable early disease detection or provide valuable insights into biology at the systems level. Most biological samples exhibit negligible magnetic susceptibility; therefore, magnetic nanoparticles have been used for diverse applications including biosensing, magnetic separation, and thermal ablation therapy. This review focuses on the use of magnetic nanoparticles for detection of biomolecules and cells based on magnetic resonance effects using a general detection platform termed diagnostic magnetic resonance (DMR). DMR technology encompasses numerous assay configurations and sensing principles, and to date magnetic nanoparticle biosensors have been designed to detect a wide range of targets including DNA/mRNA, proteins, enzymes, drugs, pathogens, and tumor cells. The core principle behind DMR is the use of magnetic nanoparticles as proximity sensors that modulate the spin-spin relaxation time of neighboring water molecules, which can be quantified using clinical MRI scanners or benchtop nuclear magnetic resonance (NMR) relaxometers. Recently, the capabilities of DMR technology were advanced considerably with the development of miniaturized, chip-based NMR (μNMR) detector systems that are capable of performing highly sensitive measurements on microliter sample volumes and in multiplexed format. With these and future advances in mind, DMR biosensor technology holds considerable promise to provide a high-throughput, low-cost, and portable platform for large scale molecular and cellular screening in clinical and point-of-care settings. *WIREs Nanomed Nanobiotechnol* 2010 2 291–304

The development of robust, versatile, and high-throughput biosensing platforms is expected to have far-reaching implications in medicine, point-of-care clinical diagnostics, pharmaceutical drug development, and genomic and proteomic research. Enabled by rapidly emerging nanotechnologies (nanoparticles, nanotubes, and nanowires) and microfabrication techniques (MEMS, microfluidics, and CMOS), several new sensing platforms have been proposed and tested for biomedical applications.[1–9] Despite these inroads, there remains a need to develop practical assay methodologies that (1) have higher sensitivity and specificity, (2) can minimize sample preparation, (3) can measure widely different types of molecules using the same format and instrument and (4) can be run in single tube point-of-care or high-throughput screening formats. These stringent prerequisites are necessary for translation to clinical settings, because molecular measurements will have to be performed on smaller and smaller samples to enable multiplexing and longitudinal monitoring so that treatment strategies can be tailored to individual patients in real time.

Biosensing strategies based on magnetic nanoparticles have received considerable attention because they offer unique advantages over other techniques. For example, magnetic nanoparticles are inexpensive to produce, physically and chemically stable, biocompatible, and environmentally safe. In addition, biological samples exhibit virtually no magnetic background, and thus highly sensitive measurements can be performed in turbid or otherwise visually obscured samples without further processing. Optical techniques on the other hand are often affected by scattering, absorption,

*Correspondence to: rweissleder@mgh.harvard.edu

Center for Systems Biology, Massachusetts General Hospital, Harvard Medical School, Boston, MA 02114, USA

DOI: 10.1002/wnan.84

and/or autofluorescence within the sample. To date, numerous methods have been developed to sense biomolecules using magnetic labels.[10] These include techniques that use magnetometers, such as SQUID,[11,12] magnetoresistive sensors,[13–20] and Hall sensors[21] to directly detect magnetic particles. Another method that has achieved considerable success is based on magnetic resonance (MRI/NMR), which involves using magnetic nanoparticles as proximity sensors to accelerate the relaxation rate of neighboring water molecules. This technique is analogous to magnetic resonance imaging, which is used to look inside the human body, and as such has been dubbed diagnostic magnetic resonance (DMR). DMR assays employ affinity molecule-conjugated magnetic nanoparticles to bind molecular targets and induce a change in proton relaxation rate using one of two different procedural 'modes'. The first involves tagging large structures such as whole cells, and requires a subsequent wash step to remove unbound nanoparticle sensors. The second mode makes use of the phenomenon of magnetic relaxation switching (MRSw), in which molecular targets are used to assemble magnetic nanoparticles into clusters and thereby affect a corresponding change in the bulk relaxation rate.[22,23] In both cases, the binding interactions are performed homogeneously in solution and make use of a built-in amplification strategy invoked by the magnetic resonance effect on billions of neighboring water molecules. Therefore, DMR is faster than other magnetic detection techniques that require solid-phase immobilization, diffusion of nanoparticles to sensing elements, or discrete amplification steps. To date, DMR has successfully been used to detect a wide variety of molecular targets with high sensitivity and specificity, including DNA, mRNA, proteins, enzyme activity, metabolites, drugs, pathogens, and tumor cells (Table 1). Initially, DMR measurements were performed using clinical MRI scanners or benchtop NMR systems.[22,24] Recently, a miniaturized, chip-based NMR (μNMR) detector system was developed that houses all components for DMR detection in a handheld, portable device.[25–27] The μNMR-chip device is capable of performing measurements on microliter sample volumes and contains multiple detection coils to enable parallel sensing of numerous biomarkers, and thus represents a critical advance in DMR technology that could enable interrogation of clinical samples in point-of-care settings.

This review will cover the various aspects of DMR biosensing, including descriptions of the magnetic nanoparticles and MRI/NMR detectors employed. We will then discuss applications of DMR to molecular and cellular biosensing.

MAGNETIC RELAXATION PROPERTIES

Magnetic Relaxation Mechanism

Magnetic resonance relaxation has recently been reviewed in detail, including relaxation mechanisms and theoretical models.[43] Briefly, the nanoparticles used are superparamagnetic, becoming magnetized when placed in an external magnetic field and losing their magnetic moment when the field is removed. This phenomenon arises because the nanoparticles consist of a single crystal domain, and thus exhibit a net magnetic moment directed along an anisotropy axis. With the help of thermal energy, however, the magnetic moment can overcome the anisotropy barrier and spontaneously flip from one direction of anisotropy to another. An ensemble of magnetic nanoparticles consequently displays negligible magnetic remanence. When placed inside an external magnetic field, the magnetic moments align in the direction of the field lines and enhance the magnetic flux. This behavior is similar to paramagnetism, but since it is associated with a large particle with fixed magnetic moment it is referred to as superparamagnetism. Although subjected to an external magnetic field, each superparamagnetic nanoparticle produces a large magnetic dipole. The resulting local magnetic field gradient creates an inhomogeneity in the external magnetic field, which destroys the coherent precession of nuclear spins of neighboring water protons. The net effect is a change in magnetic resonance signal that can be quantified by magnetic resonance (MRI/NMR) techniques as a shortening of the longitudinal (or spin-lattice, T_1) and transverse (or spin–spin, T_2) relaxation times. Typically, T_2 is used for DMR biosensing applications because the transverse relaxivity (r_2) is significantly greater than r_1 for most magnetic nanoparticles. This is important because the higher the relaxivity, the fewer the number of nanoparticles that are required to produce a detectable signal.

The magnetic relaxation properties of a population of magnetic nanoparticles are not only dependent on the particle relaxivity. Instead, the organizational state of the population is also relevant, as aggregation of particles into clusters has been shown to enhance the net transverse relaxation rate ($R_2 = 1/T_2$).[22,23] This phenomenon, known as MRSw, is a cooperative process in which the direct interaction of nanoparticles causes them to more efficiently dephase the spins of neighboring protons in comparison to when

TABLE 1 | DMR Biosensing Assays Developed to Date

Type	Target	Magnetic Nanoparticle Sensor	Reference
DNA	Telomeres	$(CCCTAA)_3$-CLIO	28
RNA	GFP	CLIO-ATTTGCCGGTGT and CLIO-TCAAGTCGCACA	22
Protein	GFP	Anti-GFP-CLIO	22
	Avidin (Av)	Biotin-CLIO	25, 29
	β-HCG	Anti-HCG-CLIO	30
	Telomerase	Anti-telomerase-CLIO	31
	CA-125	Anti-CA-125-CLIO	25
	VEGF	Anti-VEGF-CLIO	25
	α-fetoprotein	Anti-α-fetoprotein-CLIO	25
Enzyme activity	Caspase-3	CLIO-Av-Biotin-GDEVDG-CLIO	22
	BamH1	CLIO-TTA-CGC-CTAGG-ATC-CTC and CLIO-AAT-GCG-GGATCC-TAC-GAG	32
	Methylase, MboI, DpnI	Methylated BamH1 sensor	32
	Renin	Biotin-IHPFHLVIHTK-Biotin; Av-CLIO	33
	Trypsin	Biotin-$(G)_4$RRRR$(G)_3$K-Biotin or Biotin-GPARLAIK-Biotin; Av-CLIO	33
	MMP-2	Biotin-GGPLGVRGK-Biotin; Av-CLIO	33
	Caspase-3	Biotin-GDEVDG-CLIO; Av-CLIO	22
	Telomerase	CLIO-AATCCCAATCCC and CLIO-AATCCCAATCCC	28, 31
	Peroxidases	Phenol-CLIO, tyrosines-CLIO	34
Small molecules	Drugs, enantiomers	D-Phenylalanine-CLIO	35
	Folate	Folate-CLIO; anti-folate	36
	Glucose	Glucose-CLIO; concavalin	36
	HA peptide	HA-CLIO; anti-HA	36
	Calcium	Calmodulin-CLIO; M13-CLIO or chelaters	37, 38
	Influenza Tag peptide	Anti-Tag-CLIO	39, 40
Organism	Herpes simplex virus	Anti-gpD(HSV-1)-CLIO; Anti-HSV1-CLIO	41
	Adenovirus-5	Anti-Adenovirus-5-CLIO	41
	MAP	Anti-MAP-CLIO	42
	S. aureus	Vancomycin-CLIO	25
	BCG/MTB	Anti-BCG-CLIO, Anti-BCG-CB	27
Cells	Tumor cell lines	Anti-Her2-CLIO; Anti-EGFR-CLIO; Anti-EpCAM-CLIO	25
	FNA (mouse xenografts)	Anti-Her2-MnMNP; Anti-EGFR-MnMNP; Anti-CD326-MnMNP	26

they are evenly dispersed (Figure 1(a)). The current hypothesis posed to explain the mechanism of relaxation switching is based on outer-sphere theory, which predicts that the relaxivity of a particle is directly proportional to the cross-sectional area.[44,45] Consequently, when nanoparticles assemble into clusters, the effective cross-sectional area increase exceeds the additive contribution from of each particle, yielding a larger and relatively more powerful magnetic dipole. The longitudinal relaxivity is not affected by clustering, and therefore r_1 can be used as a measure of total nanoparticle concentration regardless of aggregation state.[23]

DMR Assay Configurations

As indicated in Figure 1(a), MRSw assays can be designed to cause self-assembly of magnetic nanoparticles upon addition of molecular targets (forward switching, decreasing T_2) or disassembly of preformed clusters by enzymatic cleavage or competitive binding (reverse switching, increasing T_2). Forward MRSw assays are based on cross-linking magnetic nanoparticles into clusters using molecular target bridges. Thus, they are ideally suited for detecting small molecule analytes such as drugs, metabolites, oligonucleotides, and proteins because the short cross-links ensure that the magnetic

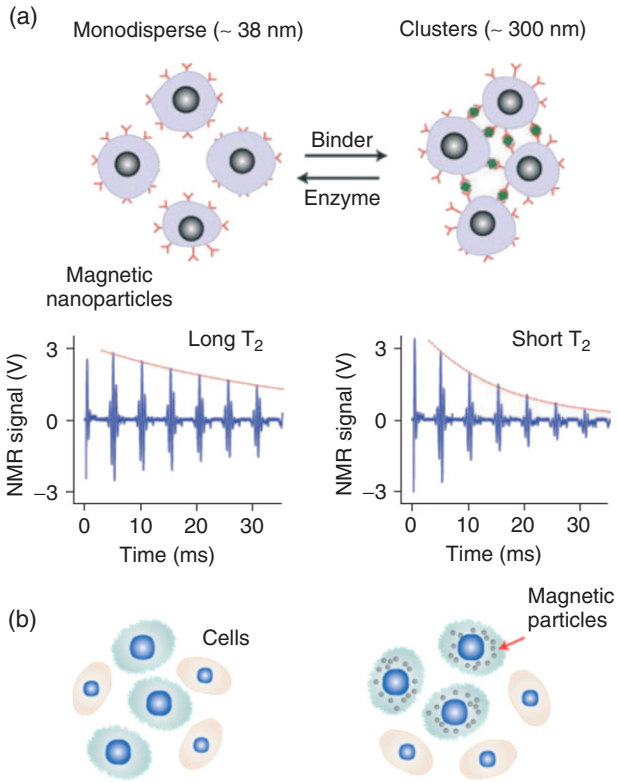

FIGURE 1 | Principles of DMR sensing assays using magnetic nanoparticles. (a) Magnetic relaxation switching assays involve assembly of magnetic nanoparticle clusters using a target biomarker as a cross-linking bridge, or disassembly of preformed clusters using an enzyme or competitive binding. Clustering magnetic nanoparticles causes them to more efficiently dephase the nuclear spins of neighboring water molecules, shortening the transverse relaxation time (T_2). Likewise, disassembly of clusters increases T_2 relaxation time. (b) Tagging cells with magnetic nanoparticles imparts a magnetic moment that is proportional to the number of nanoparticles bound. Following washing procedures to remove unbound nanoparticles, the magnetic moment can be measured as a decrease in T_2 relaxation time. (Reprinted with permission from Ref 25. Copyright 2008 Nature Publishing Group).

nanoparticles are placed in close enough proximity to promote relaxation switching. In addition, there is no need for time-consuming separation or capture strategies because MRSw assays can be performed in turbid solutions such as blood and do not require removal of unbound magnetic nanoparticles. Interestingly, increasing the valency of a target by coupling to a protein or microparticle carrier has been shown to improve detection sensitivity by a factor greater than the increase in valency.[39] This result is due to the fact that higher valency targets can more effectively promote nanoparticle clustering, liberating the MRSw technique from the equivalence principle (maximum sensitivity at equal-molar ratios of magnetic nanoparticle and target) that normally dominates. Therefore, it may be beneficial to first capture targets with a particle prior to performing the switching assay to make use of this valency effect. For reverse MRSw assays, nanoparticle clusters are first formed analogously to a forward assay before addition of an enzyme that cleaves the molecular bridges at specific sites or a competitive binding molecule that destabilize the cross-links.

Magnetic nanoparticles can also be used to tag cell surface markers and thereby impart a magnetic moment to the cell that is proportional to the number of nanoparticles bound (Figure 1(b)). This method does require removal of excess magnetic nanoparticles prior to measuring T_2 relaxation time, however, but this can readily be accomplished by centrifugation or filtration. The magnetic tagging concept has been widely employed for high-contrast MR imaging.

MAGNETIC NANOPARTICLES

Magnetic nanoparticles used for DMR sensing should ideally have a strong magnetic moment to induce pronounced T_2 changes while also exhibiting superparamagnetic behavior to avoid spontaneous magnetic aggregation. In addition, the nanoparticles must be passivated with a hydrophilic and biocompatible coating to prevent aggregation in aqueous solution and provide a means to attach affinity molecules such as antibodies, DNA, or peptides. Finally, smaller nanoparticles are advantageous because they typically exhibit higher solution stability (no sedimentation) and, for cell labeling applications, can pack more closely to maximize surface coverage.

Cross-linked Iron Oxide Nanoparticles

Cross-linked iron oxide (CLIO) nanoparticles have predominantly been used for DMR biosensing applications because they have excellent biological properties.[46] CLIO nanoparticles contain a superparamagnetic iron oxide core [3–5 nm sized monocrystalline iron oxide nanoparticles (MION)] composed of ferrimagnetic magnetite (Fe_3O_4) and/or maghemite (γFe_2O_3). Maghemite is structurally and functionally similar to magnetite but differs in that it contains cation vacancies in the sublattice. The iron oxide core is coated with dextran that is successively treated with epichlorohydrin to form stabilizing cross-links and ammonia to provide primary amine group functionality. Aminated CLIO (amino-CLIO) nanoparticles have an average hydrodynamic diameter of 25–40 nm and approximately 40–80 amines available per particle for conjugation of biomolecules.[47] The amine

groups can then be reacted with various reagents to attach biomolecules via anhydride, amine, hydroxyl, carboxyl, thiol, or epoxide groups.[48] Bioconjugation of CLIO using copper catalyzed azide-alkyne reactions ('click chemistry') has also been reported.[49–51]

Manganese-Doped Iron Oxide Magnetic Nanoparticles

The magnetic moment of iron oxide nanoparticles can be enhanced by doping the magnetite crystal with metal ions such as manganese, cobalt, and nickel.[52] Additionally, r_2 increases proportionally with the diameter of the magnetic core.[53] These factors were recently utilized to create magnetic nanoparticles with substantially greater relaxivity for DMR applications.[26] Ferrite-based nanoparticles doped with manganese [manganese-doped iron oxide magnetic nanoparticles (Mn-MNP)] were synthesized by reacting iron (III) acetylacetonate [$Fe(acac)_3$], manganese (II) acetylacetonate [$Mn(acac)_3$] and 1,2-hexadecanediol at high temperature (300°C). A seed-growth approach was then employed to incrementally increase the size of the core crystal from 10 nm to 12, 16, and 22 nm. Mn-MNP with diameter ≤16nm were highly monodispersed, exhibited crystalline ferrite structure, and were superparamagnetic at 300 K (Figure 2(a)). In addition, magnetization was proportional to the Mn-MNP core diameter size, with r_2 values as high as 6×10^{-11} s^{-1}·(particle/ml)$^{-1}$ (300 s^{-1} mM^{-1}) at 0.5 T, which is nearly 100 times greater than CLIO on a per nanoparticle basis [0.07×10^{-11} s^{-1}·(particle/ml)$^{-1}$, or 50 s^{-1} mM^{-1}].[22] This is due in part to the larger core size, but the Mn-MNP also have an approximately sixfold higher r_2 value on a per mass basis. Assuming a one-to-one ratio of biomarker-to-magnetic nanoparticle, then it is the relaxivity per nanoparticle that is most pertinent to determining performance in DMR tagging assays. Rather than using a dextran coating like CLIO, Mn-MNP were rendered water soluble using the small molecule meso-2,3-dimercaptosuccinic acid (DMSA), which has been used extensively by other groups.[52–54] DMSA has a terminal carboxylic acid group on one end that interacts directly with the magnetic core, whereas the other end contains a sulfhydryl group that can form di-thiol cross-links with other DMSA molecules to increase stability. The remaining free sulfhydryl groups can then be used to attach biomolecules via di-thiol bonds or maleimide chemistry. Due to the small size of DMSA, the Mn-MNP nanoparticles were smaller than CLIO despite the larger magnetic core.

Elemental Iron Core/Ferrite Shell Nanoparticles ('Cannonballs')

Elemental iron (Fe) has a higher magnetization than metal oxides, and this aspect has led to creation of Fe-core magnetic nanoparticles with extremely high relaxivity.[55,56] The Fe-core must be protected from oxidation, which has been accomplished using a ferrite shell. Recently, a 16-nm Fe-core/ferrite shell magnetic nanoparticle, named Cannonballs, was developed for DMR applications (Figure 2(b)).[27] The relaxivity of

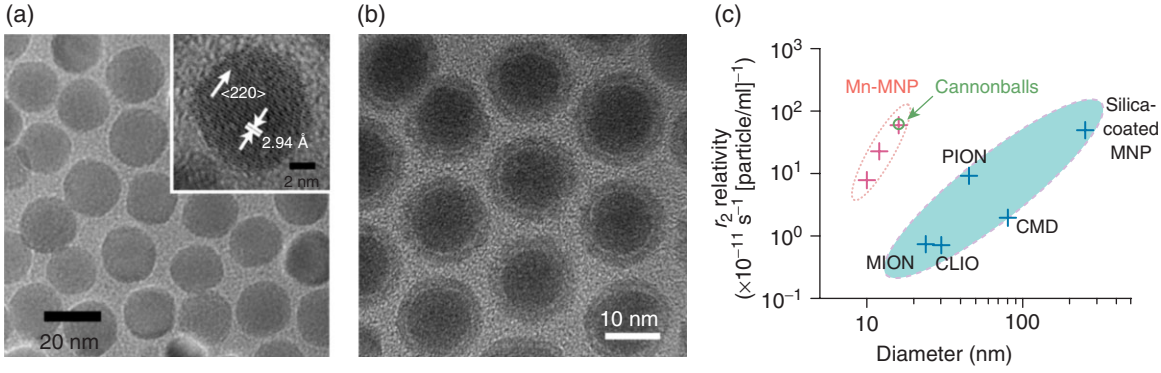

FIGURE 2 | Higher relaxivity magnetic nanoparticles developed to improve DMR detection sensitivity. (a) Transmission electron micrograph (TEM) of manganese-doped ferrite magnetic nanoparticles (Mn-MNP), demonstrating narrow size distribution and high crystallinity. The magnetic core was synthesized using a seed-growth method to produce 10, 12, 16, and 22 nm crystals. (b) TEM of elemental iron (Fe) core/ferrite shell magnetic nanoparticles ('cannonballs') with 11 nm core diameter and 2.5 nm shell thickness. The Fe-core was synthesized by thermal decomposition followed by controlled oxidation using oxygen gas to produce the ferrite shell, which protected the core from further oxidation. (c) For their size, the Mn-MNP and cannonballs exhibit higher relaxivity compared to other commercially available or reported magnetic nanoparticles. (Reprinted with permission from Ref 26. Copyright 2009 National Academy of Sciences, USA. Reprinted with permission from Ref 27. Copyright 2009 John Wiley and Sons, Inc.).

Cannonballs was similar to the Mn-MNP nanoparticles [6×10^{-11} s^{-1}·(particle/ml)[1]], which is considerably higher than other commercially available or previously reported ferrite nanoparticles when normalized for core size (Figure 2(c)). Cannonballs were synthesized by thermal decomposition of $Fe(CO)_5$ to form the Fe-core. The protective ferrite shell was then formed by controlled oxidation with oxygen gas at high temperature, which produced a thinner shell compared with the chemical oxidizers used previously.[56] Cannonballs were then coated with DMSA as described for the Mn-MNP nanoparticles.

Micrometer-Sized Magnetic Particles

Although this review is focused on the use of magnetic nanoparticles for biosensing, micrometer-scale magnetic particles have also been shown to possess certain interesting properties for MRSw assays.[40] For instance, microparticles have a higher magnetic moment because they contain considerably more Fe atoms per particle and have higher binding valency. Furthermore, placing microparticles in a magnetic field for an extended period of time induces them to cluster, which reverses when the field is removed. This magnetic field clustering has been shown to significantly enhance detection sensitivity. The large size of micrometer-scale clusters results in rapid settling out of solution; however, which complicates assay readout. Therefore, although interesting, microparticles pose significant hurdles for use as MRSw and will not be discussed further in this review. Due to their small size, Brownian motion precludes similar detection sensitivity enhancements from magnetic-field assistance for nanoparticles.

MAGNETIC RELAXATION DETECTION DEVICES

Initial Magnetic Resonance Detectors

Magnetic resonance can be detected using MRI scanners, which are used to obtain stunningly detailed images of the body, and NMR spectroscopy, which is used to study proteins and small molecules. Both of these techniques have been used to measure spin–spin relaxation time (T_2) for DMR biosensing assays. Clinical and experimental MRI scanners employ strong magnetic fields (1–11 T) generated by superconducting magnets, as well as sophisticated data acquisition schemes. In addition, parallel measurements can be obtained using multi-welled plates.[22,24,31] However, MRI scanners suffer from high operating costs, bulky equipment size (mainly due to superconducting magnets), and the need for relatively large sample volumes (hundreds of microliters). Benchtop relaxometers provide a lower cost alternative, making them more accessible for use in DMR sensing.[22,41] Benchtop systems operate at lower NMR frequencies (100 kHz–50 MHz) and are equipped with a permanent, low field (<1 T) magnet for field generation. However, benchtop systems lack the capability to perform parallel measurements and still require relatively large sample volumes.

Miniaturized NMR Chip

To overcome the limitations of available detectors, a chip-based μNMR system was recently developed to perform multiplexed DMR measurements on smaller sample volumes.[25] The μNMR system consists of microcoils for both radio-frequency (RF) excitation and NMR signal detection, an on-board NMR spectrometer, and microfluidic networks (Figure 3(a)). The magnetic field can be generated using a small, portable magnet because miniaturization lessens the need for spatial homogeneity of the magnetic field.

The first μNMR prototype was designed with planar coils that were lithographically patterned on a glass substrate.[25] The microcoils were arranged in an array format for parallel measurements, and each microcoil held 5–10 μl of sample. Subsequently, a second-generation μNMR was developed that employed solenoidal microcoils embedded in a microfluidic structure to increase the filling factor (Figure 3(b)).[26,27] This new configuration reduced the sample volume to approximately 1 μl and resulted in more homogeneous radio-frequency magnetic fields with less electrical resistance. The μNMR system is thus well suited to detect multiple targets in mass-limited biological samples and to preserve expensive reagents.

The NMR electronics, which include an RF transmitter for sample excitation and a receiver for NMR signal detection, were initially implemented using discrete components.[25] In later versions, they were monolithically integrated on a single CMOS IC chip.[57] The chip was designed to overcome the adverse conditions for NMR measurement stemming from system miniaturization including: (1) low NMR signal levels from small sample volumes and (2) fast signal decay (large T_2*) due to field inhomogeneity caused by the portable magnet. These limitations were overcome by implementing low noise RF amplifiers with high voltage gain and development of an on-chip digital pulse generator for spin-echo (Carr–Purcell–Meiboom–Gill, CPMG) sequences. Proton relaxation times were measured

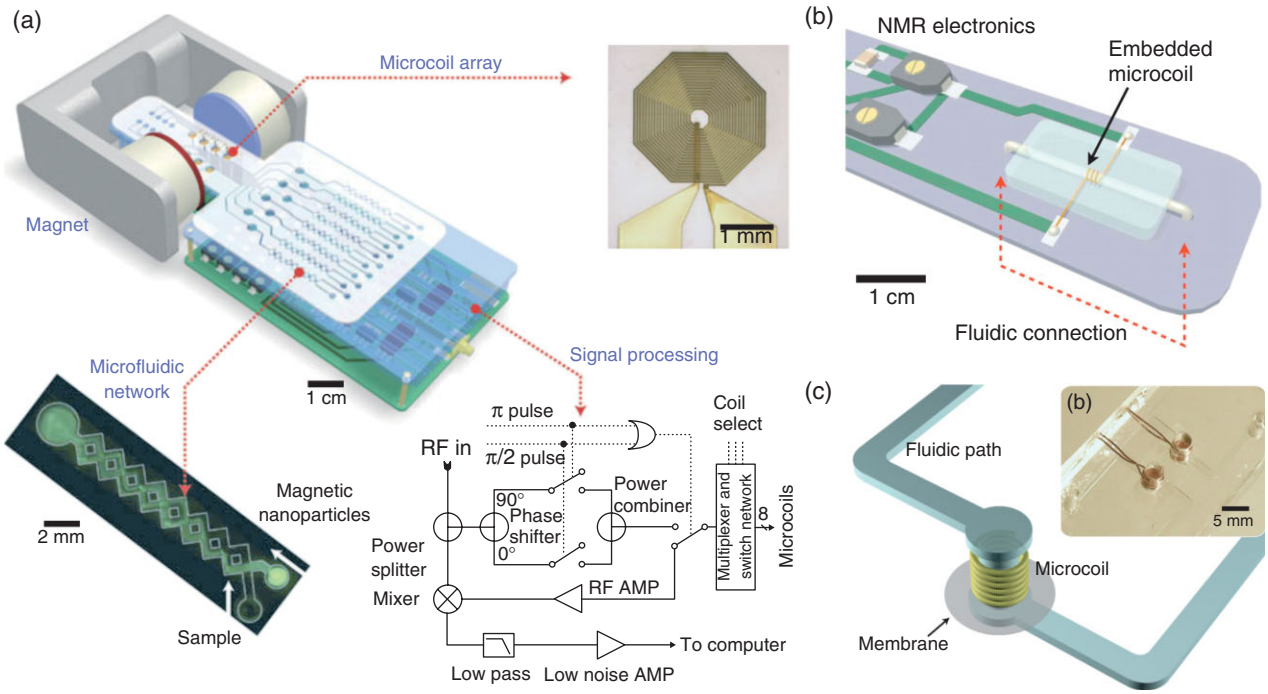

FIGURE 3 | Schematic diagram of the miniaturized NMR device developed for DMR. (a) The original system, consisting of an array of planar microcoils for NMR measurements, microfluidic networks for sample handling and mixing, miniaturized NMR electronics, and a small, portable magnet for polarizing magnetic field generation. Insets depict (clockwise) a planar microcoil, schematic of the NMR electronics, and a microfluidic mixing network. (b) The second-generation μNMR with solenoidal coil embedded in a PDMS microfluidic network, which increased filling factor, reduced signal-to-noise ratio, and decreased the required sample volume to ~ 1 μl. The probe was mounted along with all NMR electronics on a single CMOS IC chip. (c) Depiction of a membrane filter that can be mounted at the coil outlet, enabling concentration of large samples (i.e., cells) and removal of smaller impurities. (Reprinted with permission from Ref 25. Copyright 2008 Nature Publishing Group. Reprinted with permission from Ref 26. Copyright 2009 National Academy of Sciences, USA. Reprinted with permission from Ref 27 Copyright 2009 John Wiley and Sons, Inc.).

using inversion recovery pulse sequences (T_1) and CPMG spin-echo pulse sequences (T_2) to compensate for the inhomogeneity of the polarizing magnetic field.

The microfluidic networks facilitate the handling and distribution of small sample volumes, mix different flow streams and confine the sample to the most sensitive region of a given microcoil. In addition, a membrane filter can be included at the outlet of the solenoidal microcoils to size-selectively retain large species such as cells and remove smaller contaminants such as unbound magnetic nanoparticles, thus making it possible to concentrate cells from large sample volumes and to perform washing steps on-chip (Figure 3(c)).[27]

The entire NMR platform can be packaged as a handheld unit for portable, point-of-care operations. Furthermore, benchmarking against conventional NMR systems indicated that the detection sensitivity was comparable, but came at substantially reduced sample size requirement and device cost. Table 2 contains a summary of the various magnetic resonance detectors discussed.

DMR SENSING APPLICATIONS USING MAGNETIC NANOPARTICLES

Nucleotides

The concept of MRSw was first demonstrated using oligonucleotides.[22,23] Two separate CLIO nanoparticle biosensors were prepared by attaching different complimentary 12 base pair oligonucleotides that recognized adjacent sites on a 24 base pair target sequence. Addition of the target oligonucleotide sequence resulted in rapid (<30 min) nanoparticle aggregation and a subsequent decrease in T_2 relaxation time. The change in T_2 varied linearly with the amount of target added, and the detection sensitivity threshold was shown to be in the sub-femtomole range (Figure 4(a)). The nanoparticle assemblies could be dissociated by heating, and T_2 changes were similar when the experiment was performed in a turbid solution. Moreover, no change in T_2 was observed when scrambled oligonucleotide sequences were used, but inclusion of even a single mismatch in the target sequence resulted in a detectable signal change relative to the perfectly

TABLE 2 | Magnetic Resonance Detectors Used for DMR Assays

Platform	Size	Microfluidics	Multiplexing	Vol	Cost ($)	Reference
Clinical MRI	Room	None	Yes	~1 ml	2 M	22,28,34
Experimental MRI	Room	None	Yes	>300 µl	500 k	31
NMR relaxometer	Benchtop	None	No	>300 µl	50 k	22,28,31
µNMR-1 (planar coils, discrete ICs)	Handheld	Mixing	Yes	10 µl	100	25
µNMR-2 (Solenoidal coils, CMOS IC)	Handheld	Mixing, Filter	Yes	~ 1µl	100	26,27,57

matched sequence. This technique may therefore prove valuable for mutational analysis. Finally, dose-dependent detection of GFP mRNA from whole cell lysates was demonstrated.[22]

Proteins

MRSw biosensors were originally developed to detect soluble proteins by leveraging the specificity of antibodies. The first example involved detection of GFP protein to establish a proof-of-principle.[22] GFP-sensitive CLIO was prepared by first conjugating with avidin, followed by attachment of biotinylated anti-GFP polyclonal antibody. Using this system, GFP was rapidly (<30 min) detected in a dose-dependent manner down to the low femtomole range (Figure 4(b)). Addition of BSA protein did not elicit a change in T_2. In a different study, a slightly different strategy was employed to detect the beta subunit of human chorionic gonadotrophin (HCG-β), a biomarker implicated in prostate and ovarian cancers.[30] In this case, two different monoclonal antibodies that bind disparate, non-overlapping epitopes on the HCG-β protein were attached to separate CLIO nanoparticle populations. HCG-β was successfully detected using this system in a dose-dependent manner, and the sensitivity improved when an HCG dimer was used as the target and the number of antibodies per CLIO nanoparticle was increased. Recently, MRSw biosensors capable of detecting the tumor markers CA-125, VEGF, and α-fetoprotein were described and used for parallel detection of each marker in blood using the µNMR device.[25]

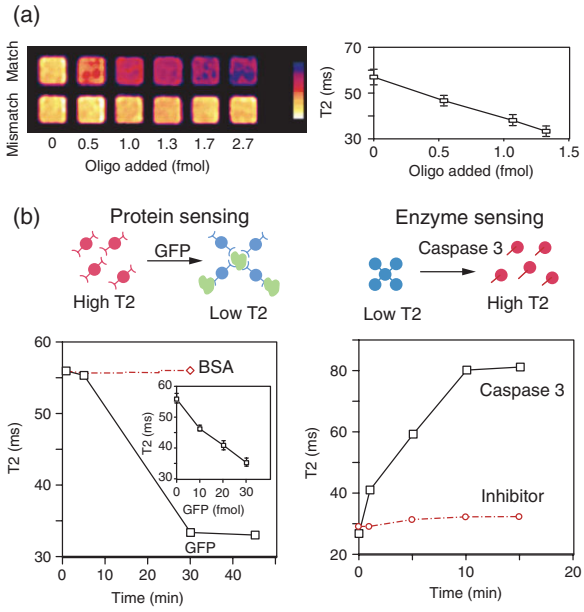

FIGURE 4 | Detection of oligonucleotides, protein, and enzyme activity using MRSw sensors. (a) T_2-weighted MR image of a 384-well plate containing varying amounts (0.5–2.7 fmol) of target or mismatched oligonucleotide and constant levels of two magnetic nanoparticle populations conjugated with different oligonucleotides complimentary to the target. Formation of nanoparticle clusters by hybridization with the target resulted in a reduction in T_2 relaxation time that varied linearly with the amount of target added. (b) Magnetic nanoparticles conjugated with a polyclonal antibody specific for GFP were incubated with GFP protein or BSA as a control. T_2 relaxation time decreased linearly with protein concentration, attaining a steady state within 30 min. (c) Magnetic nanoparticles were clustered using a linker containing the peptide sequence DEVD and were rapidly (~10 min) dissociated upon addition of caspase-3 enzyme, resulting in an increase in T_2 relaxation time. (Reprinted with permission from Ref 22. Copyright 2002 Nature Publishing Group).

Enzyme Activity

The MRSw assay strategy that lends itself most readily to the detection of enzymatic activity is the disassembly of preformed clusters due to direct action of the enzyme. Such reverse sensors have been designed to detect protease[58] and endonuclease/methylase[32] activities. In the first case, MRSw aggregates were formed using the peptide sequence biotin-GDEVDGC, which was attached to an avidin-conjugated CLIO population via the biotin and a second CLIO population using the thiol provided by the terminal cysteine. Addition of caspase-3 disassembled the aggregates by cleaving within the DEVD site, leading to a corresponding increase in T_2 relaxation time (Figure 4(c)). A similar strategy was used to create trypsin, renin, and matrix metalloproteinase 2 sensors.[33] Moreover, endonuclease activity was detected by clustering CLIO with complimentary DNA strands containing a BamHI cleavage

site, followed by the addition of BamHI enzyme. Similarly, methylase activity was detected using the methylated and non-methylated forms of the BamHI sensor and the methylation-sensitive enzymes DpnI and MboI.

Assembly of nanoparticle sensors by the product of an enzyme reaction has also been demonstrated. For instance, MRSw were designed to assess human telomerase (hTERT) activity by recognition of the 30-base pair telomeric repeat sequences in complimentary fashion (Figure 5(a)).[28] These nanoparticle sensors where subsequently used to determine telomerase activity in cell lysates from numerous tumor lines and to test the efficacy of telomerase inhibitors. Recently, a dual-nanosensor system that separately sensed telomerase activity and the total amount of hTERT protein was employed that helped elucidate the link between hTERT phosphorylation and enzymatic activity (Figure 5(b) and (c)).[31] This finding could have important implications for anti-telomerase therapies. Finally, myeloperoxidase (MPO) sensors were designed by attaching phenol-containing molecules (dopamine or serotonin) to CLIO.[34] In the presence of peroxidase, tyroxyl radicals are formed that homogeneously react to form o,o-dityrosine cross-links between the nanoparticles. Leukocyte-derived MPO has been shown to be critical to the pathogenesis of atherosclerotic plaques through oxidation of LDL and other proteins,[59,60] making these sensors a potentially useful diagnostic tool for patients with heart disease.

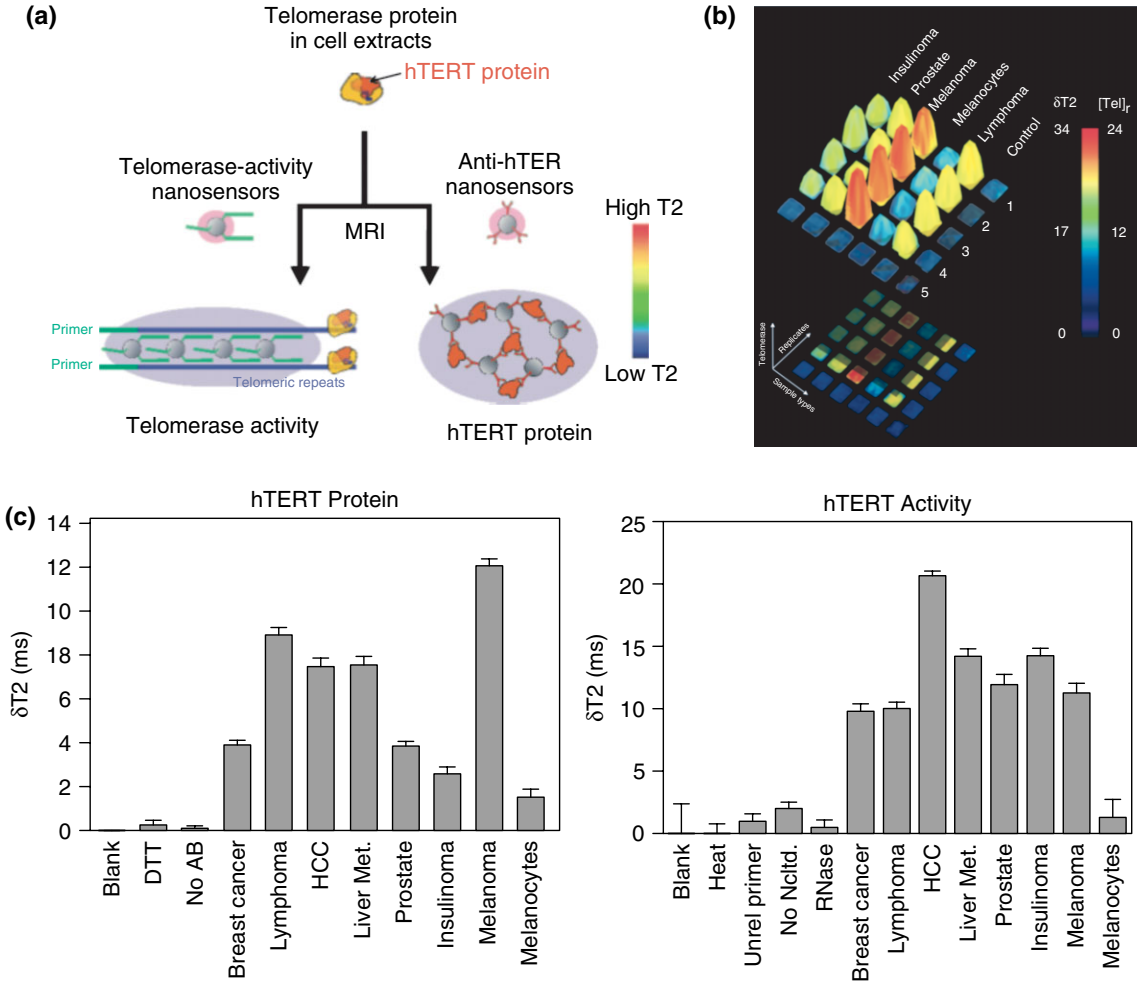

FIGURE 5 | Dual MRSw sensor system to detect human telomerase (hTERT) protein and activity levels. (a) Schematic depicting the two magnetic nanoparticle sensors, which hybridize with the 30-base pair telomeric repeat sequences (hTERT activity) or bind the hTERT protein directly using a polyclonal antibody. (b) Detection of hTERT protein in cell lysates from various cell types by MR imaging. (c) Parallel detection of hTERT protein and activity in cell lysates, demonstrating the lack of correlation between protein and activity levels. (Reprinted with permission from Ref 56. Copyright 2008 Neoplasia Press, Inc.).

Small Molecules

MRSw sensors for small molecules operate best under the disassembly paradigm because they are not large enough to contain multiple non-overlapping epitopes. Instead, a competitive binding strategy is useful, as demonstrated for glucose, folic acid, and the influenza hemagglutinin peptide (HA).[36] Here the small molecules themselves were first attached to CLIO nanoparticles, followed by cluster formation using Concavalin A (glucose) or an antibody (folic acid, HA). Addition of free analyte then led to disaggregation and a concomitant increase in T_2 time. Importantly, the change in T_2 was reversible, as removal of analyte resulted in reassembly of the nanoparticles. This led to construction of a semi-permeable membrane device capable of sensing analyte concentration in real time over numerous cycles of addition and removal.[36] Recently, a similar implantable device was developed to constantly monitor HCG levels using the MRSw sensors described in the protein detection section.[61,62] The device consists of a hollow cylinder reservoir made of high-density polyethylene that is covered on one side by a semi-permeable polycarbonate membrane. The membrane functions to retain the HCG-specific nanoparticle biosensors within the device whereas allowing free passage of HCG.

MRSw sensors capable of specifying between enantiomeric drugs has also been described.[35] Finally, pro-aggregation schemes have been developed to detect calcium by making use of specific chelators[37] and the calcium-dependent interaction between calmodulin and the M13 peptide derived from rabbit myosin light chain kinase.[38]

Pathogens

Intact organisms such as viruses and bacteria have successfully been detected using antibody-conjugated MRSw sensors. This is interesting because these targets are on the same order of size or even considerably larger than the magnetic nanoparticles. For example, adenovirus-5 and herpes simplex virus-1 were detected by polyclonal antibody-conjugated CLIO in serum with a lower limit of five viral particles in 10 μl.[41] Likewise, the bacterium *Mycobacterum avium* spp. *paratuberculosis* (MAP), which is difficult to culture and identify using current detection methods, was successfully detected using MRWs in mixtures of other bacteria and in complex fluids such as milk and blood.[42] The detection limit was on the order of 100 colony-forming units (CFUs). Detection of the bacterium *Staphylococcus aureus* was recently demonstrated using the μNMR device, where the low sample volume requirement (10 μl) enabled detection of as few as 10 CFUs.[25]

Another study was aimed at detecting tuberculosis (TB) bacterium via the cell tagging method.[27] Standard TB diagnostic tests are performed on sputum samples, and involve detection by either culture or acid-fast bacilli (AFB) smear microscopy. To mimic this process, the bacillus Calmette-Guerin (BCG), which was used as a surrogate for *Mycobacterium tuberculosis*, was spiked into sputum samples, liquefied by the standard protocol, and incubated with magnetic nanoparticles conjugated with an anti-BCG monoclonal antibody. Unbound magnetic nanoparticles were then removed within the second-generation μNMR device fitted with a porous membrane filter (~100 nm size cut-off). The membrane allowed passage of the nanoparticles but not BCG, enabling concentration of BCG from larger volumes of sample and removal of unbound nanoparticles (Figure 6(a)). In this manner, approximately 100 CFUs could be detected in 1 μl sample volumes using CLIO nanoparticles, and this improved to about 6 CFUs using the more highly magnetic Fe-core/ferrite shell nanoparticles (cannonballs) (Figure 6(b)). Finally, using the membrane filter to concentrate larger sample volumes, it was demonstrated that as few as 20 CFUs could be detected in a 1-ml sputum sample. This detection threshold is significantly greater than the AFB smear microscopy technique employed for TB detection and was comparable to the culture technique but required minutes rather than weeks.

Tumor Cell Detection and Profiling

Molecular profiling of the tumor cell surface markers Her2/neu, EGFR, and CD326 (EpCAM) was recently demonstrated using the first generation μNMR device.[25] CLIO nanoparticles were conjugated with monoclonal antibodies to each target, followed by incubation with breast cancer cells lines or fibroblasts as a control. After centrifugal washing steps, significant differences in T_2 relaxation time were observed for cancer cells compared with controls using as few as 1000 cells in a 10-μl sample volume. Detection sensitivity was significantly improved using the second-generation μNMR device, which enabled detection of Her2/neu from as few as 200 breast cancer cells in a 1-μl sample volume using CLIO nanoparticles (Figure 7(a)).[26] Notably, the detection threshold was further reduced to approximately two cells by using the more magnetic Mn-MNP (Figure 7(b)). Comparison of DMR measurements

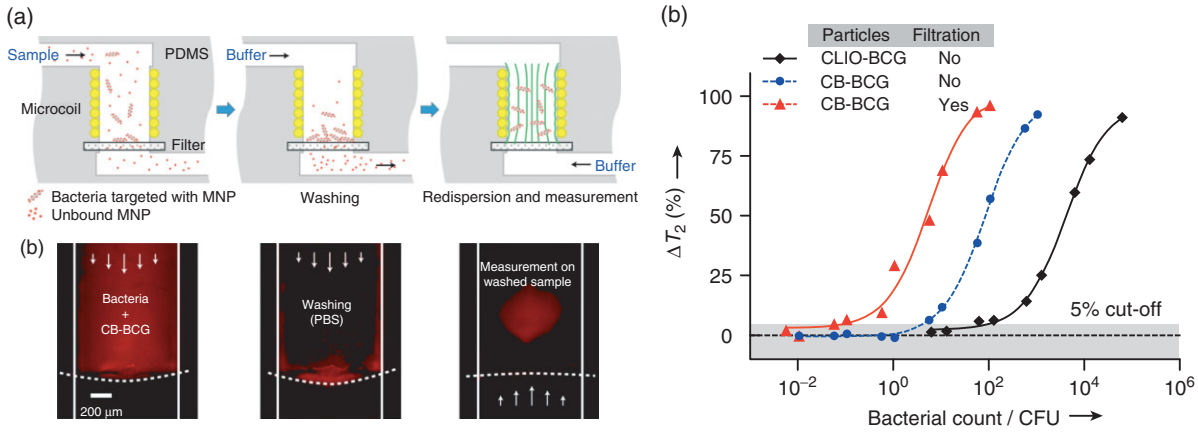

FIGURE 6 | Detection of tuberculosis (TB) bacteria using the µNMR device by tagging cells with magnetic nanoparticles. (a) Using a membrane filter mounted at the outlet of the microcoil probe, bacterial samples could be concentrated, washed of excess magnetic nanoparticles, and resuspended prior to measurement of T_2 relaxation time. (b) Detection threshold was approximately 100 colony-forming units (CFUs) using CLIO nanoparticles and 6 CFUs using the higher relaxivity cannonball nanoparticles. Sensitivity was increased to ~1 CFU in 1 ml of sample using filtration. (Reprinted with permission from Ref 27. Copyright 2009 John Wiley and Sons, Inc.).

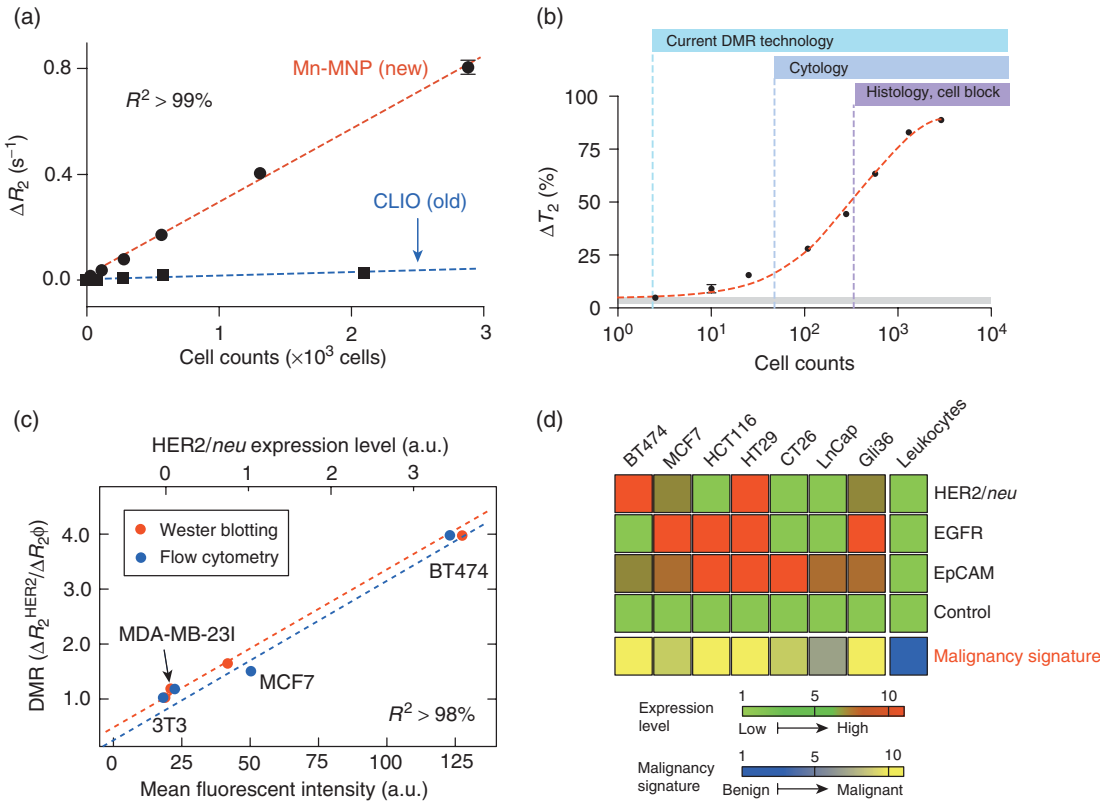

FIGURE 7 | Tumor cell detection and profiling using the µNMR device. (a) Her2/neu was detected on the surface of the breast cancer cell line BT474 using anti-Her2 CLIO and Mn-MNP nanoparticles. The change in R_2 varied linearly with cell number, and detection sensitivity was greater using the more magnetic Mn-MNP. (b) Detection threshold was approximately two cells in the 1-µl sample volume using the Mn-MNP nanoparticles. (c) DMR results correlated well with other molecular detection techniques (Western blot and flow cytometry), but required substantially fewer cells. (d) Profiling of fine-needle aspirates obtained from a panel of mouse tumor xenografts for the cancer markers Her2/neu, EGFR, and EpCAM. A control particle was used as an estimate of cell concentration based on non-specific phagocytosis. Use of the three-marker approach increased the success rate of a correct cancer 'diagnosis'. (Reprinted with permission from Ref 26. Copyright 2009 National Academy of Sciences, USA).

obtained from screening numerous breast cancer cell lines for Her2/neu expression to results from flow cytometry and Western blot indicated close correlation (Figure 7(c)). Thus, DMR is useful not only for specific cell detection but also to quantify the amount of marker per cell, while using orders of magnitude fewer cells (10–100 for DMR, 10^4–10^5 for flow cytometry, 10^5–10^6 for Western blot) than other techniques. It should be noted that the determination of marker expression level requires an estimate for the total number of cells present to differentiate between a high expression level on few cells and low expression on many cells. This can be accomplished by measuring the signal from a sample incubated with a control nanoparticle, which will be slowly taken up into the cells by phagocytosis. Since the rate of magnetic nanoparticle phagocytosis is relatively constant for epithelial tumor cells, cell number can then be estimated based on a calibration curve. Finally, fine-needle aspirate biopsies from a panel of mouse xenograft tumors were successfully analyzed for Her2/neu, EGFR, and EpCAM expression, and the multiple marker detection strategy was shown to significantly improve the likelihood of a positive cancer diagnosis (Figure 7(d)). Given the growing interest in utilizing molecular information to customize and monitor cancer therapies, magnetic tagging and detection using the μNMR device could provide a powerful tool for analyzing cells from sample-limited sources such as fine-needle aspirate biopsies or circulating tumor cells.[63,64]

CONCLUSION

DMR is a powerful biosensor technology that offers unique advantages over other detection techniques, such as a homogeneous assay format, built-in amplification scheme, broad applicability to profile different types of targets (DNA, proteins, metabolites, and cells) using different modes of operation, minimal sample preparation requirement, ability to perform measurements in obscure/turbid media, and high-throughput capacity. The technology could thus have broad applications in biomedicine, including genomics/proteomics, cancer biology, and systems biology. For instance, there is currently considerable interest in developing a better understanding of rare cell populations such as circulating tumor cells in the blood or cancer stem cells. Through the development of the chip-based μNMR device, the ability to molecularly characterize these important cells is coming closer to a reality. With further advances such as more sophisticated on-board sample processing or purifications, this device could also facilitate translation of DMR into the clinic or other point-of-care settings to aid in diagnosis of a myriad of diseases and formulation of individualized therapies. Notably, the low cost and portability of the device could help make inroads in developing countries to help in the battle against serious public health issues such as tuberculosis and HIV. Finally, as evidenced by the implantable HCG sensor, ingenuity should open up additional avenues for DMR sensing that yet remain untapped.

ACKNOWLEDGEMENTS

The authors acknowledge funding support from the National Institutes of Health (U01-HL080731, U54-CA119349 and R01-EB004626).

REFERENCES

1. Aebersold R, Mann M. Mass spectrometry-based proteomics. *Nature* 2003, 422:198–207.

2. Aslan K, Lakowicz JR, Geddes, CD. Plasmon light scattering in biology and medicine: new sensing approaches, visions and perspectives. *Curr Opin Chem Biol* 2005, 9:538–544.

3. Heath JR, Davis ME. Nanotechnology and cancer. *Annu Rev Med* 2008, 59:251–265.

4. Nam JM, Thaxton CS, Mirkin CA. Nanoparticle-based bio-bar codes for the ultrasensitive detection of proteins. *Science* 2003, 301:1884–1886.

5. Patolsky F, Timko BP, Yu G, Fang Y, Greytak AB, et al. Detection, stimulation, and inhibition of neuronal signals with high-density nanowire transistor arrays. *Science* 2006, 313:1100–1104.

6. Schroder L, Lowery TJ, Hilty C, Wemmer DE, Pines A. Molecular imaging using a targeted magnetic resonance hyperpolarized biosensor. *Science* 2006, 314:446–449.

7. Stern E, Klemic JF, Routenberg DA, Wyrembak PN, Turner-Evans DB, et al. Label-free immunodetection with CMOS-compatible semiconducting nanowires. *Nature* 2007, 445:519–522.

8. Zheng G, Patolsky F, Cui Y, Wang WU, Lieber CM. Multiplexed electrical detection of cancer markers with nanowire sensor arrays. *Nat Biotechnol* 2005, 23:1294–1301.
9. Sha MY, Xu H, Natan MJ, Cromer R. Surface-enhanced Raman scattering tags for rapid and homogeneous detection of circulating tumor cells in the presence of human whole blood. *J Am Chem Soc* 2008, 130:17214–17215.
10. Tamanaha CR, Mulvaney SP, Rife JC, Whitman LJ. Magnetic labeling, detection, and system integration. *Biosens Bioelectron* 2008, 24:1–13.
11. Kotitz R, Matz H, Trahms L, Koch H, Weitshies W, et al. SQUID based remanence measurements for immunoassays. *IEEE Trans Appl Superconduct* 1997, 7:3678–3681.
12. Chemla YR, Grossman HL, Poon Y, McDermott R, Stevens R, et al. Ultrasensitive magnetic biosensor for homogeneous immunoassay. *Proc Natl Acad Sci USA* 2000, 97:14268–14272.
13. Baselt DR, Lee GU, Natesan M, Metzger SW, Sheehan PE, et al. A biosensor based on magnetoresistance technology. *Biosens Bioelectron* 1998, 13:731–739.
14. Graham DL, Ferreira HA, Freitas PP, Cabral JM. High sensitivity detection of molecular recognition using magnetically labelled biomolecules and magnetoresistive sensors. *Biosens Bioelectron* 2003, 18:483–488.
15. Li G, Sun S, Wilson RJ, White RL, Pourmand N, et al. Spin valve sensors for ultrasensitive detection of superparamagnetic nanoparticles for biological applications. *Sens Actuators A Phys* 2006, 126:98–106.
16. Parkin SS, Kaiser C, Panchula A, Rice PM, Hughes B, et al. Giant tunnelling magnetoresistance at room temperature with MgO (100) tunnel barriers. *Nat Mater* 2004, 3:862–867.
17. Brzeska M, Panhorst M, Kamp PB, Schotter J, Reiss G, et al. Detection and manipulation of biomolecules by magnetic carriers. *J Biotechnol* 2004, 112:25–33.
18. Osterfeld SJ, Yu H, Gaster RS, Caramuta S, Xu L, et al. Multiplex protein assays based on real-time magnetic nanotag sensing. *Proc Natl Acad Sci USA* 2008, 105:20637–20640.
19. Graham DL, Ferreira H, Bernardo J, Freitas PP, Cabral JMS. Single magnetic microsphere placement and detection on-chip using current line designs with integrated spin valve sensors: biotechnological appliations. *J Appl Phys* 2002, 91:7786–7788.
20. Wang SX, Bae SY, Li G, Sun S, White RL, et al. Towards a magnetic microarray for sensitive diagnostics. *J Magn Magn Mater* 2005, 293:731–736.
21. Aytur T, Foley J, Anwar M, Boser B, Harris E, et al. A novel magnetic bead bioassay platform using a microchip-based sensor for infectious disease diagnosis. *J Immunol Methods* 2006, 314:21–29.
22. Perez JM, Josephson L, O'Loughlin T, Hogemann, D, Weissleder R. Magnetic relaxation switches capable of sensing molecular interactions. *Nat Biotechnol* 2002, 20:816–820.
23. Josephson L, Perez JM, Weissleder R. Magnetic nanosensors for the detection of oligonucleotide sequences. *Angew Chem Int Ed Engl* 2001, 40:3204–3206.
24. Hogemann D, Ntziachristos V, Josephson L, Weissleder R. High throughput magnetic resonance imaging for evaluating targeted nanoparticle probes. *Bioconjug Chem* 2002, 13:116–121.
25. Lee H, Sun E, Ham D, Weissleder R. Chip-NMR biosensor for detection and molecular analysis of cells. *Nat Med* 2008, 14:869–874.
26. Lee H, Yoon TJ, Figueiredo JL, Swirski FK, Weissleder R. Rapid detection and profiling of cancer cells in fine-needle aspirates. *Proc Natl Acad Sci USA* 2009, 106:12459–64.
27. Lee H, Yoon TJ, Weissleder R. Ultrasensitive detection of bacteria using core-shell nanoparticles and an NMR-filter system. *Angew Chem Int Ed Engl* 2009, 48:5657–5660.
28. Grimm J, Perez JM, Josephson L, Weissleder R. Novel nanosensors for rapid analysis of telomerase activity. *Cancer Res* 2004, 64:639–643.
29. Taktak S, Sosnovik D, Cima MJ, Weissleder R, Josephson L. Multiparameter magnetic relaxation switch assays. *Anal Chem* 2007, 79:8863–8869.
30. Kim GY, Josephson L, Langer R, Cima MJ. Magnetic relaxation switch detection of human chorionic gonadotrophin. *Bioconjug Chem* 2007, 18:2024–2028.
31. Perez JM, Grimm J, Josephson L, Weissleder R. Integrated nanosensors to determine levels and functional activity of human telomerase. *Neoplasia* 2008, 10:1066–1072.
32. Perez JM, O'Loughin T, Simeone FJ, Weissleder R, Josephson L. DNA-based magnetic nanoparticle assembly acts as a magnetic relaxation nanoswitch allowing screening of DNA-cleaving agents. *J Am Chem Soc* 2002, 124:2856–2857.
33. Zhao M, Josephson L, Tang Y, Weissleder R. Magnetic sensors for protease assays. *Angew Chem Int Ed Engl* 2003, 42:1375–1378.
34. Perez JM, Simeone FJ, Tsourkas A, Josephson L, Weissleder R. Peroxidase substrate nanosensors for MR imaging. *Nano Lett* 2004, 4:119–122.
35. Tsourkas A, Hofstetter O, Hofstetter H, Weissleder R, Josephson L. Magnetic relaxation switch immunosensors detect enantiomeric impurities. *Angew Chem Int Ed Engl* 2004, 43:2395–2399.
36. Sun EY, Weissleder R, Josephson L. Continuous analyte sensing with magnetic nanoswitches. *Small* 2006, 2:1144–1147.

37. Taktak S, Weissleder R, Josephson L. Electrode chemistry yields a nanoparticle-based NMR sensor for calcium. *Langmuir* 2008, 24:7596–7598.
38. Atanasijevic T, Shusteff M, Fam P, Jasanoff A. Calcium-sensitive MRI contrast agents based on superparamagnetic iron oxide nanoparticles and calmodulin. *Proc Natl Acad Sci USA* 2006, 103:14707–14712.
39. Koh I, Hong R, Weissleder R, Josephson L. Nanoparticle-target interactions parallel antibody–protein interactions. *Anal Chem* 2009, 81:3618–3622.
40. Koh I, Hong R, Weissleder R, Josephson L. Sensitive NMR sensors detect antibodies to influenza. *Angew Chem Int Ed Engl* 2008, 47:4119–4121.
41. Perez JM, Simeone FJ, Saeki Y, Josephson L, Weissleder R. Viral-induced self-assembly of magnetic nanoparticles allows the detection of viral particles in biological media. *J Am Chem Soc* 2003, 125:10192–10193.
42. Kaittanis C, Naser SA, Perez JM. One-step, nanoparticle-mediated bacterial detection with magnetic relaxation. *Nano Lett* 2007, 7:380–383.
43. Gossuin Y, Gillis P, Hocq A, Vuong QL, Roch A. Magnetic resonance relaxation properties of superparamagnetic particles. *WIREs Nanomed Nanobiotechnol* 2009, 1:299–310.
44. Brooks RA. T(2)-shortening by strongly magnetized spheres: a chemical exchange model. *Magn Reson Med* 2002, 47:388–391.
45. Gillis P, Moiny F, Brooks RA. On T(2)-shortening by strongly magnetized spheres: a partial refocusing model. *Magn Reson Med* 2002, 47:257–263.
46. Harisinghani MG, Barentsz J, Hahn PF, Deserno WM, Tabatabaei S, et al. Noninvasive detection of clinically occult lymph-node metastases in prostate cancer. *N Engl J Med* 2003, 348:2491–2499.
47. Josephson L, Tung CH, Moore A, Weissleder R. High-efficiency intracellular magnetic labeling with novel superparamagnetic-Tat peptide conjugates. *Bioconjug Chem* 1999, 10:186–191.
48. Sun EY, Josephson L, Kelly KA, Weissleder R. Development of nanoparticle libraries for biosensing. *Bioconjug Chem* 2006, 17:109–113.
49. Sun EY, Josephson L, Weissleder R. 'Clickable' nanoparticles for targeted imaging. *Mol Imaging* 2006, 5:122–128.
50. Devaraj NK, Keliher EJ, Thurber GM, Nahrendorf M, Weissleder R. 18F labeled nanoparticles for in vivo PET-CT imaging. *Bioconjug Chem* 2009, 20:397–401.
51. Thorek DL, Elias DR, Tsourkas A. Comparative analysis of nanoparticle-antibody conjugations: carbodiimide versus click chemistry. *Mol Imaging* 2009, 8:221–229.
52. Lee JH, Huh YM, Jun YW, Seo JW, Jang JT, et al. Artificially engineered magnetic nanoparticles for ultrasensitive molecular imaging. *Nat Med* 2007, 13:95–99.
53. Jun YW, Huh YM, Choi JS, Lee JH, Song HT, et al. Nanoscale size effect of magnetic nanocrystals and their utilization for cancer diagnosis via magnetic resonance imaging. *J Am Chem Soc* 2005, 127:5732–5733.
54. Huh YM, Jun YW, Song HT, Kim S, Choi JS, et al. In vivo magnetic resonance detection of cancer by using multifunctional magnetic nanocrystals. *J Am Chem Soc* 2005, 127:12387–12391.
55. Miguel OB, Gossuin Y, Morales MP, Gillis P, Muller RN, et al. Comparative analysis of the 1H NMR relaxation enhancement produced by iron oxide and core–shell iron–iron oxide nanoparticles. *Magn Reson Imaging* 2007, 25:1437–1441.
56. Peng S, Wang C, Xie J, Sun S. Synthesis and stabilization of monodisperse Fe nanoparticles. *J Am Chem Soc* 2006, 128:10676–10677.
57. Liu Y, Sun N, Lee H, Weissleder R, Ham D. CMOS mini nuclear magnetic resonance sysem and its application for biomolecular sensing. *ISSCC Digest Tech Papers* 2008, 1:140–141.
58. Perez JM, Josephson L, Weissleder R. Use of magnetic nanoparticles as nanosensors to probe for molecular interactions. *Chembiochem* 2004, 5:261–264.
59. Zhang R, Brennan ML, Fu X, Aviles RJ, Pearce GL, et al. Association between myeloperoxidase levels and risk of coronary artery disease. *Jama* 2001, 286:2136–2142.
60. Brennan ML, Penn MS, Van Lente F, Nambi V, Shishehbor MH, et al. Prognostic value of myeloperoxidase in patients with chest pain. *N Engl J Med* 2003, 349:1595–1604.
61. Daniel KD, Kim GY, Vassiliou CC, Jalali-Yazdi F, Langer R, et al. Multi-reservoir device for detecting a soluble cancer biomarker. *Lab Chip* 2007, 7:1288–1293.
62. Daniel KD, Kim GY, Vassiliou CC, Galindo M, Guimaraes AR, et al. Implantable diagnostic device for cancer monitoring. *Biosens Bioelectron* 2009, 24:3252–3257.
63. Cristofanilli M, Budd GT, Ellis MJ, Stopeck A, Matera J, et al. Circulating tumor cells, disease progression, and survival in metastatic breast cancer. *N Engl J Med* 2004, 351:781–791.
64. Maheswaran S, Sequist LV, Nagrath S, Ulkus L, Brannigan B, et al. Detection of mutations in EGFR in circulating lung-cancer cells. *N Engl J Med* 2008, 359:366–377.

